Title	Coastal iodine emissions. 1. Release of I2 by Laminaria digitata in chamber experiments
Authors	Ashu-Ayem, Enowmbi R.;Nitschke, Udo;Monahan, Ciaran;Chen, Jun;Darby, Steven B.;Smith, Paul D.;O'Dowd, Colin D.;Stengel, Dagmar B.;Venables, Dean S.
Publication date	2012
Original Citation	ASHU-AYEM, E. R., NITSCHKE, U., MONAHAN, C., CHEN, J., DARBY, S. B., SMITH, P. D., O'DOWD, C. D., STENGEL, D. B. & VENABLES, D. S. 2012. Coastal Iodine Emissions. 1. Release of I2 by Laminaria digitata in Chamber Experiments. Environmental Science & Technology, 46, 10413-10421. http://dx.doi.org/10.1021/es204534v
Type of publication	Article (peer-reviewed)
Link to publisher's version	10.1021/es204534v
Rights	Copyright © 2012 American Chemical Society. This document is the Accepted Manuscript version of a Published Work that appeared in final form in Environmental Science and Technology, copyright © American Chemical Society after peer review and technical editing by the publisher. To access the final edited and published work see http://pubs.acs.org/doi/abs/10.1021/es204534v
Download date	2025-08-02 08:23:37
Item downloaded from	https://hdl.handle.net/10468/787

Coastal iodine emissions: Part 1. Release of I_2 by *Laminaria digitata* in chamber experiments

*Enowmbi R. Ashu-Ayem, Udo Nitschke, Ciaran Monahan, Jun Chen, Steven B. Darby, Paul D. Smith, Colin D. O'Dowd, Dagmar B. Stengel, Dean S. Venables**

Department of Chemistry and Environmental Research Institute, University College Cork, Cork, Ireland

School of Physics and Ryan Institute for Environmental, Marine and Energy Research, National University of Ireland, Galway, Galway, Ireland

Botany and Plant Science, School of Natural Sciences and Ryan Institute for Environmental, Marine and Energy Research, National University of Ireland Galway, Galway, Ireland

d.venables@ucc.ie

RECEIVED DATE (to be automatically inserted after your manuscript is accepted if required according to the journal that you are submitting your paper to)

Abstract

Tidally exposed macroalgae emit large amounts of I_2 and iodocarbons that produce hotspots of iodine chemistry and intense particle nucleation events in the coastal marine boundary layer. Current emission rates are poorly characterized, however, with reported emission rates varying by three orders of magnitude. In this study, I_2 emissions from 25 *Laminaria digitata* samples were investigated in a simulation chamber using incoherent broadband cavity-enhanced absorption spectroscopy (IBBCEAS). The chamber design allowed gradual extraction of seawater to simulate tidal emersion of algae. Samples were exposed to air with or without O_3 and to varying irradiances. Emission of I_2 occurred in four distinct stages: 1) moderate emissions from partially submerged samples; 2) a strong release by fully emerged samples; 3) slowing or stopping of I_2 release; 4) later pulses of I_2 were evident in some samples. Emission rates were highly variable and ranged from 7 to 616 pmol min^{-1} gFW^{-1} in ozone-free air, with a median value of 55 pmol min^{-1} gFW^{-1} for 20 samples.

Introduction

The observation of iodine monoxide, IO, in the marine boundary layer (MBL) over a decade ago has stimulated a resurgence of interest in the sources and chemistry of atmospheric iodine (*1*, *2, 3*). In the atmosphere, atomic iodine produced via photolysis or chemical reaction reacts rapidly with ozone (O_3) to form IO:

$$I + O_3 \rightarrow IO + O_2 \quad (1)$$

Iodine species subsequently influence the atmosphere's oxidation capacity in several ways, including catalytic destruction of O_3, and altering the OH/HO_2 and NO_2/NO ratios (*4*, *5*). Studies have further shown the importance of IO in aerosol formation of iodine oxide particles in the marine atmosphere (*6–11*).

The photolytic sources of atomic iodine in the coastal MBL were initially proposed to be photolabile iodocarbons, especially CH_2I_2 and CHIBr (*12*). These compounds are emitted by brown macroalgae following exposure to air at low tide and concentrations of iodocarbons and IO show a clear tidal signature (*13*). McFiggans et al. later suggested that I_2 released by the brown macroalgae *Saccharina latissima* and *Laminaria digitata* is the major source of iodine in temperate coastal environments (*14*). Several field and laboratory studies have subsequently confirmed large emissions of I_2 into the atmosphere from a variety of brown macroalgae (*15–17*), which are known to accumulate iodine in high concentrations (*18*). For instance, *L. digitata* contains iodine at up to 4.7% of their dry weight (*19*, *20*), providing algae with an abundant and accessible source of labile iodine species for potential chemical defence mechanisms and anti-oxidative activities (*21*, *22*). Although macroalgal coastal emissions of I_2 are probably relatively minor contributors to the global budget of atmospheric iodine, they give rise to hotspots of iodine chemistry that can alter the chemistry of the coastal MBL.

Most studies of macroalgal emissions have focused on *L. digitata* because this species is probably the strongest iodine accumulator among living organisms (*22*, *23*) and emits high levels of I_2 when exposed to ambient air (*15*, *17*, *24*), or to oxidative agents such as ozone, H_2O_2 or oligoguluronates (*22*, *25*). *L.*

digitata is common on exposed shores and inhabits the lower littoral regions. Dixneuf et al. observed that *L. digitata* emitted I_2 in an intense burst over about 20 min, followed by successive smaller pulses of I_2 (*24*). Recent studies reported a wide range of I_2 emission rates from *L. digitata* – mean values ranged from 3 to 2500 pmol min^{-1} gFW^{-1} (*15*, *16*, *25*, *26*) (where FW denotes the fresh weight of the sample) and were dependent on thallus parts (*17*). The source strength of I_2 from macroalgae is therefore a key uncertainty in the role of iodine in the coastal MBL (*3*), and an improved estimate of emissions is required to understand the contribution of macroalgal iodine emissions to local atmospheric processes. Two points should be noted in this regard. The first is that a large dataset of emission rates is necessary to account for the likely variation between individual algae. The second point is that, as tidal emersion of macroalgae is a gradual process in which different thallus parts are exposed to the atmosphere at different times, a more nuanced understanding of the I_2 emission profile during emersion is desirable.

The aim of this study was to investigate the time profile of I_2 emissions from entire specimens of *L. digitata* during emersion. This is the first iodine emission study in which algal specimens were not abruptly exposed to air from the outset, but were exposed to a simulated outgoing tide under controlled conditions in an atmosphere simulation chamber. The overall work is divided into two parts. Part 1 (the present study) deals with iodine emission profiles of *L. digitata* following emersion. Simultaneous, in-situ measurements of I_2, IO, and OIO were used to quantify the amount and rate of release of I_2 from the air-exposed algae and to put an improved estimate on the emission rate of this important biogeochemical pump of iodine. The effects of irradiance and O_3 on I_2 emissions as well on the physiological response of *L. digitata* using the chlorophyll *a* fluorescence technique (*17*) were also studied. Part 2, in the accompanying paper, describes the nucleation of iodine oxide particles above air-exposed macroalgae.

Experimental Section

Simulation chamber

Experiments were carried out in a 2.2 m^3 (~10 m^2 surface area) atmosphere simulation chamber (Figure 1a) comprising a cylindrical fluorinated ethylene propylene (FEP) bag housed inside a 2 m long enclosure. The photolysis light source was an unfiltered 2 kW xenon lamp (Rige Lighting) that produced a collimated beam above the chamber. Partial cross-sections of the beam were reflected upwards to the chamber ceiling by broadband scattering surfaces at intervals along the length of the chamber. This configuration resulted in a radiation field inside the chamber with a spatial variation of less than 20%. The lamp spectrum (400 to 850 nm, λ_{max} = 550 nm) provided a good simulation of the visible solar spectrum. The photolysis rate of I_2 in the chamber (based on the initial loss rate of I_2 in excess O_3) was 0.0075±0.0010 s^{-1}, corresponding to 6% of that at the earth's surface for a cloud-free sky and an overhead sun (1100 W m^{-2}) (*27*). The lamp was mounted externally to the chamber to reduce heating of the interior and temperature rises were modest (typically within 3°C) from the start to end of experiments. A wire mesh filter was inserted between the lamp and the chamber to attenuate the radiation field inside the chamber. All experiments were carried out with the chamber illuminated. The chamber was purged for several hours before the start of each experiment and was sufficient to reduce particle concentrations to below 1 cm^{-3} and mixing ratios of chamber gases (O_3, I_2, NO_2, IO) to below the detection limit of chamber instrumentation. The chamber was operated with a constant volume of chamber air in the experiments reported here. Ozone was added in several experiments using an ozone generator (Ozone Lab model OL80W/FM). A small fan in the chamber ensured complete mixing of chamber gases within 3 min, as determined by the time taken for the absorption of a short pulse of NO_2 to stabilize.

Instrumentation

An incoherent broadband cavity-enhanced absorption spectroscopy (IBBCEAS) system was the principle tool for analyzing the gas phase composition of the chamber (*28*, *29*). The instrument in this

work (Figure 1b) comprised two optical cavities: a blue channel (420 to 460 nm) for IO and a green channel (520 to 560 nm) for I_2 and iodine dioxide, OIO. Both channels used plano-concave dielectric mirrors separated by 199 cm. Light from a 75 W xenon arc lamp was separated into two channels using a dichroic beamsplitter, bandpass filtered, and focused into the respective optical cavities. Transmitted light was recombined in a two-way fiber and coupled into a Shamrock SR163 spectrograph with a CCD detector (Andor DU420A-BU2) cooled to -40 ºC. With a 1200-l/mm grating, the resolution of the spectrograph was 0.96 nm. Spectra were acquired over 30 s.

The mirror reflectivity spectra, $R(\lambda)$, of both channels were calibrated based on the absorption of known amounts of NO_2 (from a container of known volume and NO_2 partial pressure). Maximum mirror reflectivities were 99.93% (440 nm) and 99.97% (540 nm). The extinction coefficient, $\varepsilon(\lambda)$, was calculated from the intensity transmitted when a sample was present, $I(\lambda)$ (*30*):

$$\varepsilon(\lambda) = \left(\frac{I_0}{I} - 1 \right) \frac{1 - R(\lambda)}{L} \tag{2}$$

The intensity transmitted through the clean chamber, $I_o(\lambda)$, was recorded before introducing the sample; L is the mirror separation of 199 cm. A multivariate fit based on the differential optical absorption was used to quantify the number densities of molecular absorbers, and was similar to that described by Ball and Jones (*31*). A polynomial function accounted for the smoothly-varying extinction associated with iodine oxide particles, which were formed in high numbers in some experiments. Reference spectra for IO and OIO were obtained from Spietz et al. and Bloss et al. respectively, and convoluted to our instrument function (*32*, *33*). The absorption spectrum of I_2 was measured in the chamber and scaled to the literature absorption cross section of Saiz-Lopez et al. (*27*). The weak and constant O_2 dimer and water absorption bands were also included in the fit. The blue channel was fitted from 425 to 448 nm (Figure 2a), while the green channel was fitted over the range 530 to 550 nm (Figure 2b). Fitted spectra showed good agreement to the measured absorption spectra and accounted for all significant spectral features.

Ozone was monitored using a UV absorption monitor (2B Technologies model 202) with a sampling rate of 1 L min^{-1}. A nanoSMPS comprising a TSI Aerosol Neutralizer 3077A (Kr-85 source), a nano DMA (TSI Differential Mobility Analyzer 3085) and a condensation particle counter (TSI CPC 3025A), was used for continuous particle measurements during experiments.

Algal material and experimental design

Sporophytes of *Laminaria digitata* (Hudson) Lamouroux were harvested from Garrettstown (51° 38.57'N, 008° 35.10'W) and Roches Point (51° 47.68'N, 008° 15.17'W), Co. Cork, Ireland, during daytime low tides at the end of October 2010. Samples were similar in age, on average 1.2 m long, and free from visible epiphytes. Following sampling, algae were weighed (Table 1 and 2), labelled and stored at 12-15°C under an irradiance, E_{PAR}, of 20-30 µmol photons m^{-2} s^{-1} (400 - 700 nm) in natural seawater from the sampling site. The light-dark cycle was 12 h:12 h. The seawater was continously aerated by diffusers and replaced daily by fresh seawater. All specimens were used within seven days of collection.

For iodine emission experiments, algae were placed in a 33 L tray filled with natural seawater and moved to the center of the atmosphere simulation chamber via an inlet door located towards the bottom of the chamber. The tray was located 5 cm below the two optical cavities of the spectrometer. This transfer took less than 30 s. Samples were acclimated to experimental conditions for 10 min, i.e. to an air temperature of 22 ± 2 °C, and to 15, 100, or 235 µmol photons m^{-2} s^{-1} (light experiments), or to 15 µmol photons m^{-2} s^{-1} without or with added O_3 (O_3 experiment). Seawater in the tray was then gradually removed over a period of 5 – 10 min using a diaphragm pump and algae were exposed to air and a defined E_{PAR} for a further 70 min after emersion.(*15–17*, *24*)

In vivo chlorophyll (chl) *a* fluorescence parameters of algal samples were determined after 70 min emersion to estimate the extent of stress experienced during measurements (*34*).

Measurement of variable chlorophyll *a* fluorescence

In vivo chl *a* fluorescence parameters were measured in ambient air using a PAM fluorometer (PAM-2000, Heinz Walz) (*17*). Algae were additionally exposed to ten increasing irradiance levels (between 0 and 1160 µmol photons m^{-2} s^{-1}) provided by the internal halogen lamp of the PAM-2000. Each light level was applied for 2 min before non-photochemical quenching of chl *a* fluorescence (NPQ) was determined.

The maximum photosystem II efficiency F_v/F_m (measured after 30 min dark acclimation) was calculated as follows:

$$\frac{F_v}{F_m} = \frac{F_m - F_0}{F_m} \tag{3}$$

where F_v is the variable chl *a* fluorescence, F_m is the maximal chl *a* fluorescence after dark acclimation, and F_0 is the minimal chl *a* fluorescence.(*17*). Since differences in NPQ regulation after iodine measurements were only detected in NPQ_{max}, i.e. the NPQ value determined at 1160 µmol photons m^{-2} s^{-1}, only NPQ_{max} is presented in this study. NPQ_{max} was calculated from:

$$NPQ_{\max} = \frac{F_m - F_m'}{F_m'} \tag{4}$$

where F'_m is the maximal chl *a* fluorescence after acclimation to 1160 µmol photons m^{-2} s^{-1}.

Iodine emission studies under defined irradiances and different O_3 levels were carried out in five independent replicates (n = 5). Results of photosynthetic performance, i.e. F_v/F_m and NPQ_{max}, are shown as mean with standard deviation of n = 5 measurements on independent samples. Effects of irradiance on I_2 emission characteristics were analysed using non-parametric Kruskal Wallis H test due to high variability in obtained data. Effects of O_3 exposure on F_v/F_m and NPQ_{max} were analysed using Student's t-test. Effects of irradiance on F_v/F_m and NPQ_{max} were analysed by using 1-way ANOVA. The Tukey test identified *a posteriori* homogeneous sub-groups that differed significantly on the level of $P < 0.05$. All photosynthesis data were normally distributed (Kolmogorov–Smirnov test) and variances were homogenous (Levene test).

Results and Discussion

In vivo chlorophyll *a* fluorescence response

Physiological responses of *L. digitata* during experiments were investigated by means of chl *a* fluorescence measurements. Chl *a* fluorescence parameters such as F_v/F_m and NPQ are widely used as "health" indicators of photosynthetic active organisms and are shown in Figure 3 (*34*). F_v/F_m values of ~0.75 are typical for unstressed brown macroalgae (*35*). With increasing irradiances, mean F_v/F_m decreased significantly from 0.753 (15 µmol photons m^{-2} s^{-1}) to 0.705 (100 µmol photons m^{-2} s^{-1}) and 0.554 (235 µmol photons m^{-2} s^{-1}, $P < 0.001$, Figure 3c) showing that experimental light conditions resulted in photoinhibition, i.e. a slightly increased extent of stress experienced by the alga during emersion. This was accompanied by a reduction in NPQ_{max} from 2.735 (15 µmol photons m^{-2} s^{-1}) to 1.453 (235 µmol photons m^{-2} s^{-1}, Figure 3d) which indicates that photoprotection capacities of *L. digitata* were reduced during experiments. However, NPQ was regulated in this alga even when exposed to higher irradiances.

After exposure to air with elevated O_3, F_v/F_m values varied between 0.722 and 0.764 (Figure 3a) and were similar to values determined after exposure to O_3-free air (0.730-0.769). NPQ reflects mechanisms of non-radiative energy dissipation of excessively absorbed light energy and such mechanisms have a protective role against photoinhibition, which can be measured e.g. as a reduction in F_v/F_m (*36*). Brown macroalgae are known to exhibit high photoprotection capacities which are expressed in high NPQ values (*37*, *38*). Mean NPQ_{max} values (measured at 1160 µmol photons m^{-2} s^{-1}) were 3.726 and 3.545 after exposure to air without and with increased O_3 (Figure 3b), respectively. The fact that neither F_v/F_m nor NPQ_{max} were affected by O_3 indicates that ambient experimental conditions were not stressful enough to substantially inhibit photosynthesis.

It should be noted that the experimental light intensities and O_3 levels were within the normal range of conditions occuring in the natural habitat of *L. digitata* (*39*) but were not close to maximum natural light levels (of up to 2000 μmol photons m^{-2} s^{-1} for emerged macroalgae).

Laminaria digitata emission profiles

Typical emission profiles following emersion of *L. digitata* are presented in Figure 4 along with the smoothed instantaneous emission rates for I_2, calculated from the I_2 time profile. Mixing ratios of I_2 indicate the cumulative amount of I_2 emitted into the volume of the chamber. Overall, I_2 emissions from *L. digitata* were highly variable, ranging from 0.4 to 9.9 nmol gFW^{-1} for different specimens. Losses to chamber walls and other surfaces were small; in light of the exceptionally high variability between algae, emitted amounts of I_2 were not corrected for this minor loss and are therefore lower limits. Emissions of I_2 took place in four characteristic stages. In the first stage, modest amounts of I_2 were released from the submerged and gradually emerging alga as water was removed from the sample container. This was followed by a strong release of I_2 in the second stage, which was characterized by a sharp onset when the sample was fully exposed. This emission pulse lasted 15 to 20 min and accounted for over 80% of the emitted I_2. Emissions of I_2 then slowed or stopped completely (third stage), except in some samples, when smaller pulses of I_2 were observed after about 60 min (fourth stage).

The irradiance level had no noticeable systematic effect on the emission profiles. The irradiance was varied over an order of magnitude (15, 100 and 235 μmol photons m^{-2} s^{-1}), but was much lower than maximum daytime levels. In light of the absence of a light-induced response of I_2 emissions, these emissions are grouped together with other experiments (E_{PAR} = 15 μmol photons m^{-2} s^{-1}) in the absence of ozone.

No statistically significant effect was apparent between the mass of the alga and either the total amount of I_2 emitted, or the amount emitted per unit mass (Table 1).

Effect of Ozone

In separate experiments, 80 to 100 ppbv ozone was added to the chamber before introducing macroalgae. IO was formed as the water level was lowered and was easily observed, even at very low I_2 mixing ratios, owing to its much greater absorption cross-section than that of I_2 (Figure 5). The distinction between the stages of initial slow emission of I_2, and the much stronger subsequent release, is especially apparent from the IO mixing ratio in this figure. Strong secondary pulses of I_2 (stage 4) were observed in some samples after the main release of I_2.

The mixing ratio of IO in the chamber was limited by the fast, second-order self-reaction of IO(*40*):

$$IO + IO \rightarrow OIO + I \quad (5a)$$

$$\rightarrow I_2 + O_2 \quad (5b)$$

$$\rightarrow 2I + O_2 \quad (5c)$$

$$IO + IO + M \rightarrow IOIO + M \quad (5d)$$

Destruction of O_3 in the chamber was rapid and prompt nucleation occurred of large numbers of iodine oxide particles (*41*). OIO was not detected, however. This is a surprising finding, as OIO is a major reaction product of the IO self-reaction (5a) and is expected to be a central building block in iodine oxide particle formation (*8*, *10*, *32*, *42*, *43*). As the OIO detection limit of the spectrometer was estimated to be ca. 30 pptv (based on the fit uncertainty), rapid removal mechanisms must be operative, probably via the fast reactions of OIO with I atoms ($k = 1.1\times10^{-10}$ cm^3 molecule^{-1} s^{-1})(*44*) and IO ($k = 1.2\times10^{-10}$ cm^3 molecule^{-1} s^{-1} (*45*). Both species were present in the chamber at much higher mixing ratios than expected in the MBL: at 100 pptv IO (Figure 5), the OIO lifetime would be only 3 s.

In the presence of O_3, loss of iodine to particles via reaction (5) must be accounted for to quantify total iodine emissions. As shown in Figure 5, I_2 mixing ratios in the chamber actually decreased for a time when IO mixing ratios were high, but partly recovered once ozone was removed and IO production via reaction (1) terminated. It was not possible to estimate the amount of iodine in the aerosol phase using

measured size distributions because particles rapidly grew larger than the maximum size bin (20 nm) of the nanoSMPS. To estimate losses of I_2 to particles, the rate of reaction (5) was calculated from the measured IO concentrations. Only reactions (5a) and (5d) were assumed to result in particle formation. There is good agreement in the literature concerning the overall rate coefficient of reaction (5) (*40*), but significant differences exist in the reported branching ratios. We used the IUPAC recommended reaction rate ($k_5 = 9.9\times10^{-11}$ cm^3 molecule^{-1} s^{-1} at 298 K) and branching ratio of 0.38 for reaction (5a) at 1 bar; as the latter value was from the Bloss et al. study, we also used their value of 0.46 for the branching ratio of reaction (5d) to estimate an I_2 equivalent loss (i.e, loss of two iodine atoms to the particle phase) of $(0.5k_{5a} + k_{5d})/k_5 = 0.65$ (*33*). This value is also comparable to 0.78 obtained by Harwood et al., also at atmospheric pressure (*46*). The efficiency of iodine incorporation into particles is slightly reduced by photolysis of OIO and by thermal decomposition of I_2O_2, but this negative influence on the effective branching ratios is likely to be smaller than the uncertainty of the branching ratios, especially given the short lifetime of OIO and (presumably) of I_2O_2 (*42–44*, *47*).

Calculated total I_2 mixing ratios are shown in Figure 5 for branching ratios $(0.5k_{5a} + k_{5d})/k_5$ of 0.5, 0.65 and 0.75. Branching ratios of greater than about 0.3 removed the dip in I_2 mixing ratios and there were no abrupt changes in the slope of the I_2 mixing ratio when losses via IO terminated. Losses of iodine to particles were very large and accounted for about three quarters of the total I_2 released. Median emission rates in the presence of ozone (Table 2) were 400 pmol min^{-1} gFW^{-1} and were greater than without O_3 (65 pmol min^{-1} gFW^{-1}). However, due to the high variability this difference was not statistically significant ($P = 0.548$).

Comparison to previous emission rate measurements

This work presents the I_2 emission profiles of a comparatively large number of whole *L. digitata* displaying normal photosynthetic characteristics. An important finding of this study is that *L. digitata* emission rates of I_2 were highly variable (7 to 616 pmol min^{-1} gFW^{-1}). The range of emission rates found in this work encompasses most prior observations, and helps to reconcile the differences reported

in previous studies. These include the lower emission rates reported by Ball et al. and Palmer et al., as well as the much higher values found by Bale et al. and Nitschke et al. (*15*–*17*, *25*). For a single, whole alga, Ball et al. found a mean I_2 release rate of 3.2 pmol min^{-1} gFW^{-1}, while air-exposed samples of sections from the same alga emitted at 3.0 and 2.2 pmol min^{-1} gFW^{-1} (*16*). Palmer and co-workers reported similar hourly mean emission rates, ranging from below their detection limit to 9 pmol min^{-1} gFW^{-1} (*25*). As the bulk of I_2 emissions from *L. digitata* occur on a shorter timescale than 1 h (*15*–*17*), the Palmer et al. estimates should be revised upwards by a factor of 2 to 4 for direct comparability with other studies (*25*). With the exception of the one whole alga in Ball et al., both studies most likely investigated samples of the thalli from the distal blade, which has been shown by Nitschke et al. to emit up to 17 times less iodine compared to the stipe (*16*, *17*). Dramatically higher emission rates of ca. 2500 pmol min^{-1} gFW^{-1} were observed by Bale et al. for a single, unstressed alga (*15*). Nitschke et al. also observed high emission rates, including median values between 20 and 629 pmol min^{-1} gFW^{-1} within the first 30 min of emersion (recalculated from Nitschke et al. where *L. digitata* samples were shown to contain 83% water) (*17*). These two studies used undivided specimens, which could partly explain the large variability in emission rates.

The time dependence of the main I_2 release from fully exposed algae reported here is consistent with prior studies, with most emission occurring over a period of about 20-40 min. Smaller amounts of I_2 were released during the gradual emersion of the alga. Based on the extremely large differences between emission rates from stipes and those for distal blades, the small initial emission (stage one) is probably from the distal blades and meristematic area, which are expected to be exposed first. The strong emission in the second stage probably arises from the subsequent emergence of the stipe. Further pulses of I_2 were also observed to follow the main release event in several instances, displaying the same sporadic behavior seen by Dixneuf and co-workers over several hours, and also by Ball et al. in some samples (*16*, *24*). Our results are also consistent with the observations of Nitschke et al. that relatively low light intensities had no significant effect on the emissions (Table 1) (*17*).

The rate and duration of emission of I_2 appeared to increase markedly when algae were exposed to approximately 100 ppbv O_3 (median emission rate of 400 pmol min^{-1} gFW^{-1}). However, the sample size for O_3 experiments was insufficient to determine whether or not this result was significant. Similar observations have been reported in other studies which showed increased emissions of I_2 in the presence of O_3 or other stress factors (*16*, *20*, *25*). For instance, Ball et al. found emission rates of up to 386 pmol min^{-1} gFW^{-1}, and Palmer et al. measured rates of 130 pmol min^{-1} gFW^{-1} averaged over 1 h (*16*, *25*). The effect was more modest here, possibly owing to the larger data set and relatively low levels of oxidant, consistent with the correlation between O_3 and I_2 mixing ratios near Mace Head found by Huang and co-workers (*48*). If this correlation is robust, emission rates in the MBL would be somewhat lower than our observations.

Finally, the findings of this study can be related to the release of I_2 during the gradual emergence of *L. digitata* during low tide. During tidal retreat, the distal blades would emerge first, with increasingly longer sections floating at the surface. Small amounts of I_2 would be likely owing to the relatively lower emissions associated with the blades and because the blades would still be significantly covered by seawater, corresponding to the first emission stage observed in this work. As the stipe gradually emerged with the receding tide (in some cases held proud of the sea surface), much stronger release of I_2 would be expected This release is likely to extend over the duration of the progressive exposure of the stipe. Agitation from wave action could also stimulate greater release of I_2, as Bale et al. found (*15*). Clearly, I_2 emissions from *L. digitata* depend strongly on the particular population density and distribution of these macroalgae at a given location. For example, younger plantlets were shown to retain iodine in higher concentrations than older speciments which may result in a higher emission rate. It should be noted that our study did not address the influence of the season, temperature, age, or health on I_2 emissions by *L. digitata*. As the irradiance levels had no noticeable impact on the emitted amount or rate of I_2, we calculate a combined (n=20) median emission rate of 55 pmol min^{-1} gFW^{-1} and a median amount emitted of 3.0 nmol gFW^{-1}.

ACKNOWLEDGMENT

We thank Science Foundation Ireland for supporting this research through grants 07/RFP/GEOF716 and 09/RFP/CAP2509. UN gratefully appreciates financial support through the Irish Research Council for Science, Engineering and Technology (IRCSET “Embark Initiative”).

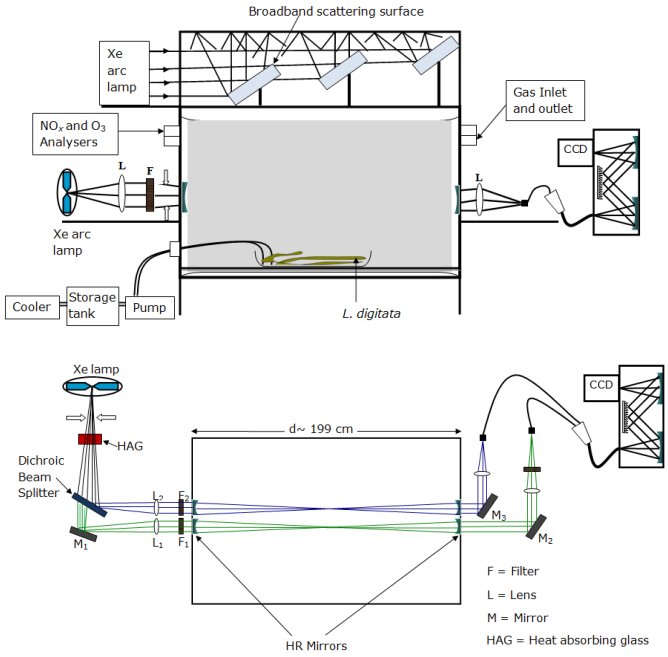

Figure 1. Schematic diagram of the simulation chamber. TOP: side view of the chamber showing the location of the sample; BOTTOM: view from above showing the two-channel IBBCEAS system.

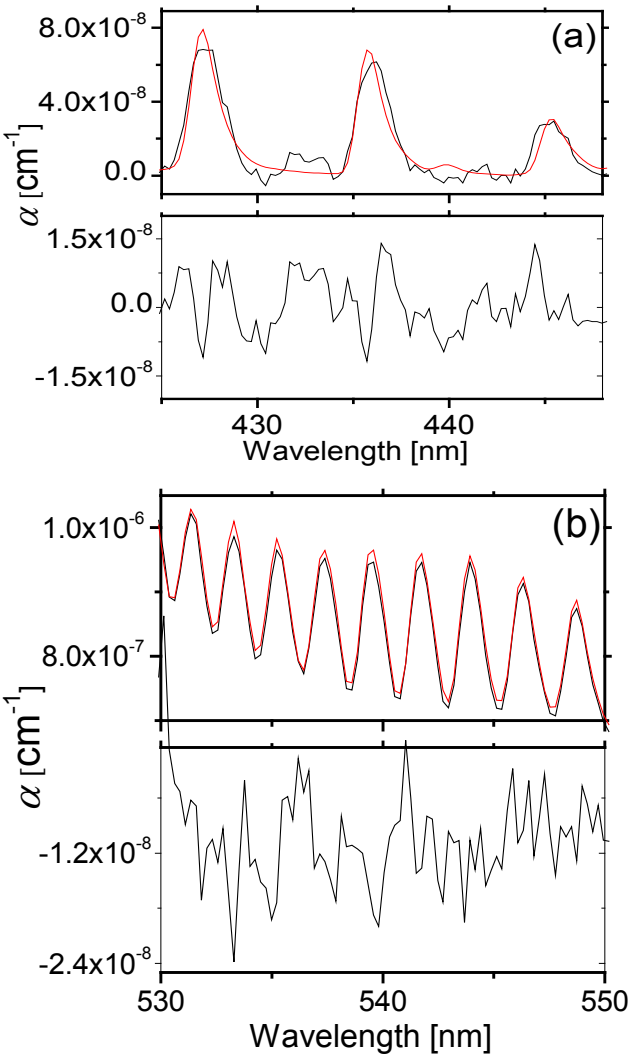

Figure 2. The measured absorption in the chamber (black) and fit of the reference spectra (red) for (a) IO and (b) I_2. The fit residual is shown below each spectrum.

Table 1. Molecular iodine (I_2) emission characteristics of *L. digitata* exposed to ambient air at 22 ± 2°C and defined irradiances E_{PAR} of 15, 100, and 235 µmol photons m^{-2} s^{-1}. Each experiment was carried out in five replicates (n=5). Significant effects of E_{PAR} on I_2 emission characteristics were analysed using the non-parametric Kruskal-Wallis test; *P* values are given. FW: fresh weight. DW: dry weight

Replicate	FW (DW) [g]	Total I_2 emitted [nmol]	Amount I_2 emitted [nmol gFW^{-1}]	Duration of emission [min]	Average emission rate [pmol min^{-1} gFW^{-1}]	Maximum emission rate [nmol min^{-1}]
Low E_{PAR} (15 µmol photons m^{-2} s^{-1})						
#1	400 (66.6)	1129	2.82	55	51.3	62.0
#2	436 (79.8)	511	1.17	55	21.3	27.0
#3	272 (44.2)	1158	4.26	63	67.6	107.8
#4	374 (66.4)	1323	3.54	60	59.0	86.3
#5	248 (40.4)	243	0.98	58	16.9	15.3
Median		**1129**	**2.82**		**51.3**	**62.0**
Medium E_{PAR} (100 µmol photons m^{-2} s^{-1})						
#6	311 (48.2)	1366	4.39	60	73.2	138.4
#7	380 (65.9)	1804	4.75	55	86.3	230.1
#8	272 (42.6)	1743	6.41	55	116.5	231.0
#9	253 (42.2)	97	0.38	55	7.0	7.2
#10	303 (49.9)	233	0.77	55	14.0	30.6
Median		**1366**	**4.39**		**73.2**	**138.4**
High E_{PAR} (235 µmol photons m^{-2} s^{-1})						
#11	360 (57.9)	1114	3.10	60	51.6	73.7
#12	425 (62.2)	602	1.42	60	23.6	51.2
#13	306 (43.6)	360	1.18	55	21.4	25.2
#14	330 (54.7)	1681	5.09	60	84.9	185.1
#15	335 (51.25)	3296	9.84	60	164	278.6
Median		**1114**	**3.10**		**51.6**	**73.7**
***P* value**		0.811	0.613		0.651	0.619

Table 2. Molecular iodine (I_2) emission characteristics of *L. digitata* exposed to ambient air without and with added O_3 at 22 ± 2°C. Each experiment was carried out in five replicates (n=5). Significant effects of O_3 on I_2 emission characteristics were analysed using the non-parametric Kruskal-Wallis test; *P* values are given. FW: fresh weight. DW: dry weight.

Replicate	FW (DW) [g]	Total I_2 emitted [nmol]	Amount I_2 emitted [nmol gFW^{-1}]	Duration of emission [min]	Average emission rate [pmol min^{-1} gFW^{-1}]	Maximum emission rate [nmol min^{-1}]
No O_3 added						
#16	355 (78.7)	476	1.34	65	20.6	21.6
#17	238 (45.7)	351	1.47	63	23.4	22.5
#18	676 (153.9)	3065	4.53	70	64.8	273.2
#19	229 (53.6)	1385	6.05	60	100.8	107.8
#20	185 (49.8)	6832	36.93	60	616.0	422.4
Median		**1385**	**4.53**		**64.8**	**107.8**
O_3 added						
#21	274 (53.7)	157	0.57	58	9.9	2.7
#22	175 (34.6)	1681	9.60	65	147.7	57.5
#23	213 (47.7)	7891	37.05	62	597.5	116.8
#24	197 (43.6)	6210	31.52	70	450.3	192.3
#25	171 (35.1)	5473	32.01	80	400.0	263.3
Median		**5473**	**31.52**		**400.0**	**116.8**
***P* value**		0.548	0.421		0.548	0.841

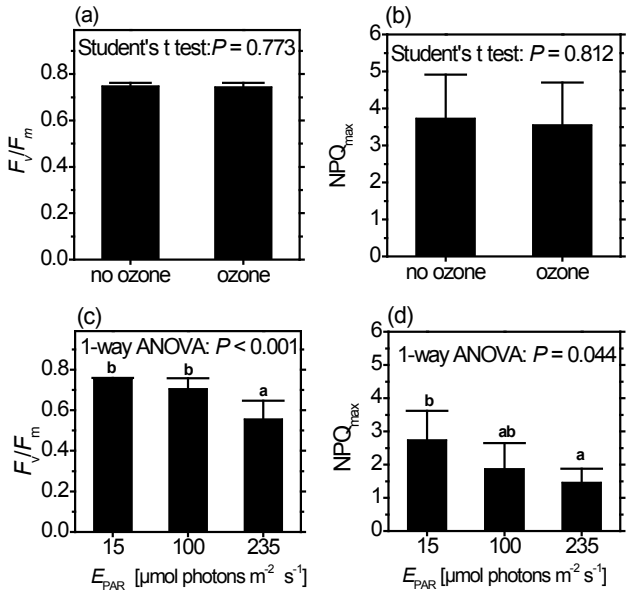

Figure 3. Effect of varying ozone levels on (a) the maximum photosystem II efficiency F_v/F_m and (b) the maximum non-photochemical quenching of chl *a* fluorescence NPQ_{max} (measured at 1160 µmol photons m^{-2} s^{-1}) of *Laminaria digitata* during 70 min exposure to air. The influence of defined irradiances E_{PAR} on F_v/F_m and NPQ_{max} are similarly presented in (c) and (d), respectively. Data are presented as mean and standard deviation (n=5). Significant effects of O_3 on photosynthetic parameters were analysed by using Student's t test; effects of E_{PAR} were analysed by using 1-way ANOVA. *P* values are given. Letters above the bars indicate significant differences within groups (i.e. between each level of E_{PAR}) as revealed by Tukey's post hoc test.

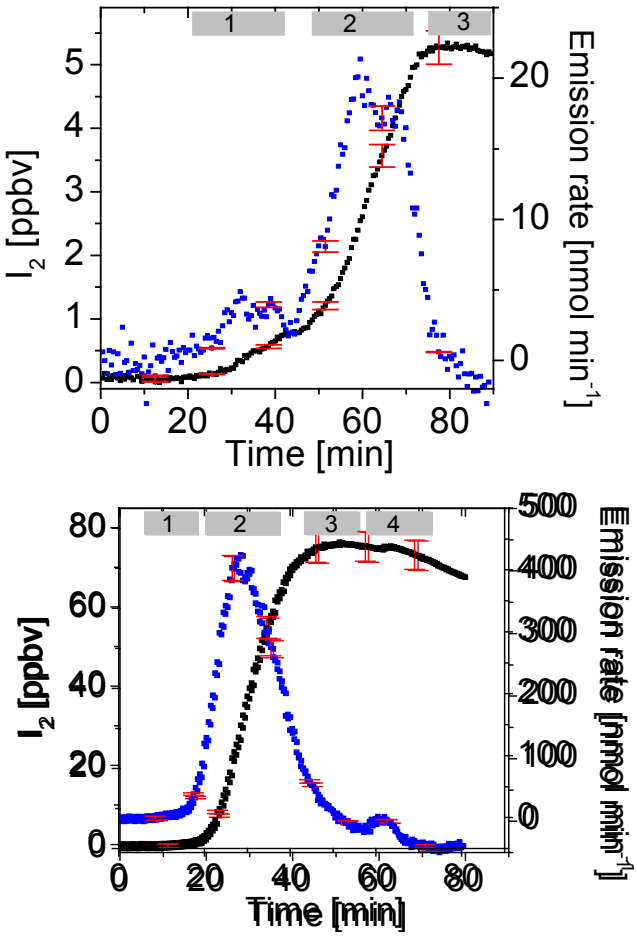

Figure 4. Iodine emission profiles (black) and calculated rate of emission (blue) of two *L. digitata*. The four stages of the iodine emission profile are shown in the grey shaded area above the plot. The error bars are shown in red.

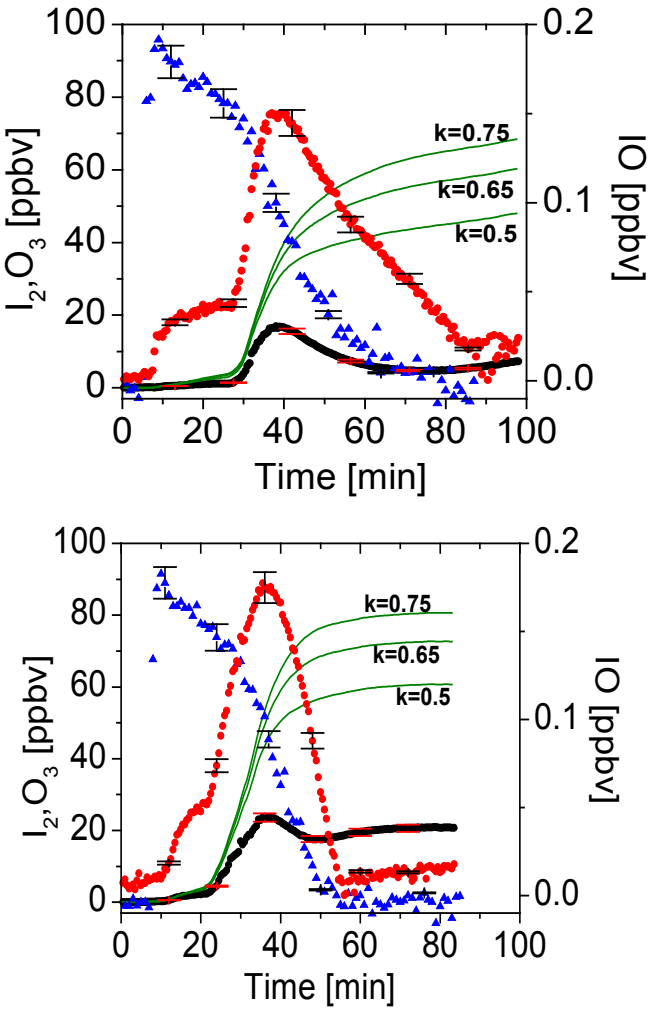

Figure 5. Time profiles of the mixing ratios of I_2 (black dots), O_3 (blue triangles) and IO (red dots, right axis) in the chamber following exposure of two specimens of *L. digitata*. The calculated total I_2 emission is shown for three different branching ratios of the IO self-reaction (green lines) leading to formation of iodine oxide particles.

Reference

(1) Alicke, B.; Hebestreit, K.; Stutz, J.; Platt, U. Iodine oxide in the marine boundary layer. *Nature* **1999**, *397*, 572-573.

(2) Allan, J.; McFiggans, G. B.; Plane, J. M. C.; Coe, H. Observations of iodine monoxide in the remote marine boundary layer. *J. Geophys. Res.* **2000**, *105*, 14363-14369.

(3) Saiz-Lopez, A.; Plane, J. M. C.; Baker, A. R.; Carpenter, L. J.; von Glasow, R.; Gómez-Martín, J. C.; McFiggans, G. B.; Saunders, R. W. Atmospheric Chemistry of Iodine. *Chem. Rev.* **2012**, *112*, 1773-1804.

(4) McFiggans, G. B.; Plane, J. M. C.; Allan, J.; Carpenter, L. J.; Coe, H.; O'Dowd, C. D. A modelling study of iodine chemistry in the marine boundary layer. *J. Geophys. Res. Atmos* **2000**, *105*, 14371-14385.

(5) Vogt, R.; Sander, R.; von Glasow, R.; Crutzen, P. J. Iodine Chemistry and its Role in Halogen Activation and Ozone Loss in the Marine Boundary Layer : A Model Study. *J. Atmos. Chem.* **1999**, *1*, 375-395.

(6) O'Dowd, C. D.; Jimenez, J.; Bahreini, R.; Flagan, R. C.; Seinfeld, J. H.; Hameri, K.; Pirjola, L.; Kulmala, M.; Jennings, S. G.; Hoffmann, T. Marine aerosol formation from biogenic iodine emissions. *Nature* **2002**, *417*, 632–636.

(7) O'Dowd, C. D.; Yoon, Y. J.; Junkerman, W.; Aalto, P.; Kulmala, M.; Lihavainen, H.; Viisanen, Y. Airborne measurements of nucleation mode particles I: coastal nucleation and growth rates. *Atmos. Chem. Phys.* **2007**, *7*, 1491-1501.

(8) Pirjola, L.; O'Dowd, C. D.; Yoon, Y. J.; Sellegri, K. Modelling Iodine Particle Formation and Growth from Seaweed in a Chamber. *Environ. Chem.* **2005**, *2*, 271-281.

(9) Saiz-Lopez, A.; Plane, J. M. C.; McFiggans, G. B.; Williams, P. I.; Ball, S. M.; Bitter, M.; Jones, R. L.; Hongwei, C.; Hoffmann, T. Modelling molecular iodine emissions in a coastal marine environment: the link to new particle formation. *Atmos. Chem. Phys.* **2005**, *5*, 5405-5439.

(10) Saunders, R. W.; Kumar, R.; Gómez-Martín, J. C.; Mahajan, A. S. Studies of the formation and growth of aerosol from molecular iodine precursor. *Phys. Chem.* **2010**, *224*, 1095-1117.

(11) Sellegri, K.; Yoon, Y. J.; Jennings, S. G.; O'Dowd, C. D.; Pirjola, L.; Cautenet, S.; Chen, H.; Hoffmann, T. Quantification of coastal new ultra-fine particles formation from in situ and chamber measurements during the BIOFLUX campaign. *Environ. Chem.* **2005**, *2*, 260-270.

(12) Carpenter, L. J.; Sturges, W. T.; Penkett, S. A.; Liss, P. S.; Alicke, B.; Hebestreit, K.; Platt, U. Short-lived alkyl iodides and bromides at Mace Head, Ireland: Links to biogenic sources and halogen oxide production. *J. Geophys. Res.* **1999**, *104*, 1679-1689.

(13) Saiz-Lopez, A.; Plane, J. M. C. Novel iodine chemistry in the marine boundary layer. *Geophys. Res. Lett.* **2004**, *31*, 1999-2002.

(14) McFiggans, G. B.; Coe, H.; Burgess, R.; Allan, J.; Cubison, M.; Rami Alfarra, M.; Saunders, R. W.; Saiz-Lopez, A.; Plane, J. M. C.; Wevill, D.; Carpenter, L. J.; Rickard, A. R.; Monks, P. S.

Direct evidence for coastal iodine particles from Laminaria macroalgae – linkage to emissions of molecular iodine. *Atmos. Chem. Phys.* **2004**, *4*, 701-713.

(15) Bale, C. S. E.; Ingham, T.; Commane, R.; Heard, D. E.; Bloss, W. J. Novel measurements of atmospheric iodine species by resonance fluorescence. *J. Atmos. Chem.* **2008**, *60*, 51-70.

(16) Ball, S. M.; Hollingsworth, A. M.; Humbles, J.; Leblanc, C.; Potin, P.; McFiggans, G. B. Spectroscopic studies of molecular iodine emitted into the gas phase by seaweed. *Atmos. Chem. Phys.* **2010**, *10*, 6237-6254.

(17) Nitschke, U.; Ruth, A. A.; Dixneuf, S.; Stengel, D. B. Molecular iodine emission rates and photosynthetic performance of different thallus parts of Laminaria digitata (Phaeophyceae) during emersion. *Planta* **2011**, *233*, 737-48.

(18) Saenko, N. G.; Kravtsova, Y. Y.; Ivanenko, V. V.; Sheludko, S. I. Concentration of iodine and Bromine by plants in the seas of Japan and Okhotsk. *Marine Biology* **1978**, *47*, 243 - 250.

(19) Ar Gall, E.; Küpper, F. C.; Kloareg, B. A survey of iodine content in Laminaria digitata. *Botanica Marina* **2004**, *47*, 30-37.

(20) Küpper, F. C.; Schweigert, N.; Ar Gall, E.; Legendre, J.-M.; Vilter, H.; Kloareg, B. Iodine uptake in Laminariales involves extracellular, haloperoxidase-mediated oxidation of iodide. *Planta* **1998**, *207*, 163-171.

(21) Verhaeghe, E. F.; Fraysse, A.; Guerquin-Kern, J.; Wu, T.; Devès, G.; Mioskowski, C.; Leblanc, C.; Ortega, R.; Ambroise, Y.; Potin, P. Microchemical imaging of iodine distribution in the brown alga Laminaria digitata suggests a new mechanism for its accumulation. *J. Biol. Inorg. Chem.* **2008**, *13*, 257-269.

(22) Küpper, F. C.; Carpenter, L. J.; McFiggans, G. B.; Palmer, C. J.; Waite, T. J.; Boneberg, E.; Woitsch, S.; Weiller, M.; Abela, R.; Grolimund, D.; Potin, P.; Butler, A.; Luther, G. W.; Kroneck, P. M. H.; Meyer-Klaucke, W.; Feiters, M. C. Iodide accumulation provides kelp with an inorganic antioxidant impacting atmospheric chemistry. *PNAS* **2008**, *105*, 6954-6958.

(23) Küpper, F. C.; Feiters, M. C.; Olofsson, B.; Kaiho, T.; Yanagida, S.; Zimmermann, M. B.; Carpenter, L. J.; Luther, G. W.; Lu, Z.; Jonsson, M.; Kloo, L. Commemorating two centuries of iodine research: An interdisciplinary overview of current research. *Angew. Chem., Int. Ed. Engl.* **2011**, 11598-11620.

(24) Dixneuf, S.; Ruth, A. A.; Vaughan, S.; Varma, R. M.; Orphal, J. The time dependence of molecular iodine emission from Laminaria digitata. *Atmos. Chem. Phys.* **2009**, *9*, 823-829.

(25) Palmer, C. J.; Anders, T. L.; Carpenter, L. J.; Küpper, F. C.; McFiggans, G. B. Iodine and halocarbon response of Laminaria digitata to oxidative stress and links to atmospheric new particle production. *Environ. Chem.* **2005**, *2*, 282-290.

(26) Kundel, M.; Thorenz, U. R.; Petersen, J. H.; Huang, R.-J.; Bings, N. H.; Hoffmann, T. Application of mass spectrometric techniques for the trace analysis of short-lived iodine-containing volatiles emitted by seaweed. *Anal. Bioanal. Chem.* **2012**, *402*, 3345-3357.

(27) Saiz-Lopez, A.; Saunders, R. W.; Joseph, D. M.; Ashworth, S. H.; Plane, J. M. C. Absolute absorption cross-section and photolysis rate of I_2. *Atmos. Chem. Phys.* **2004**, *4*, 1443-1450.

(28) Gherman, T.; Venables, D. S.; Vaughan, S.; Orphal, J.; Ruth, A. A. Incoherent broadband cavity-enhanced absorption spectroscopy in the near-ultraviolet: application to HONO and NO_2. *Environ. Sci. Technol.* **2008**, *42*, 890-895.

(29) Chen, J.; Wenger, J. C.; Venables, D. S. Near-ultraviolet absorption cross sections of nitrophenols and their potential influence on tropospheric oxidation capacity. *J. Phys. Chem. A* **2011**, *115*, 12235-12242.

(30) Fiedler, S. E.; Hese, A.; Ruth, A. A. Incoherent broad-band cavity-enhanced absorption spectroscopy. *Chem. Phys. Lett.* **2003**, *371*, 284-294.

(31) Ball, S. M.; Jones, R. L. Broadband cavity ring-down spectroscopy. In *Cavity Ring-Down Spectroscopy: Techniques and Applications, edited by: Berden, G. and Engel, R.*; Blackwell Publishing Ltd, 2009; Vol. 103, pp. 5239-5262.

(32) Spietz, P.; Gómez-Martín, J. C.; Burrows, J. P. Spectroscopic studies of the I_2/O_3 photochemistry Part 2. Improved spectra of iodine oxides and analysis of the IO absorption spectrum. *Photochem. Photobiol. A* **2005**, *176*, 50-67.

(33) Bloss, W. J.; Rowley, D. M.; Cox, R. A.; Jones, R. L. Kinetics and products of the IO self-reaction. *J. Phys. Chem. A* **2001**, *105*, 7840-7854.

(34) Maxwell, K.; Johnson, G. N. Chlorophyll fluorescence-a practical guide. *Botany* **2000**, *51*, 659-668.

(35) Büchel, C.; Wilhelm, C. In vivo analysis of slow fluorescence induction kinetics in algae: progress, problems and perspectives. *J Photochem. Photobiol.* **1993**, *58*, 137-148.

(36) Horton, P.; Ruban, A. Molecular design of the photosystem II light-harvesting antenna: photosynthesis and photoprotection. *Botany* **2005**, *56*, 365-373.

(37) Harker, M.; Berkaloff, C.; Lemoine, Y.; Britton, G.; Young, A.; Duval, J. C.; Rmiki, N.-E.; Rousseau, B. Effects of high and desiccation on the operation of xanthophyll cycle in two marine brown algae. *European Journal of Physology* **1999**, *34*, 35-42.

(38) Gevaert, F.; Créach, A.; Davoult, D.; Holl, A. C.; Seuront, L.; Lemoine, Y. Photo-inhibition and seasonal photosynthetic performance of the seaweed Laminaria saccharina during a simulated tidal cycle: chlorophyll fluorescence measurements and pigment analysis. *Plant, Cell Environ.* **2002**, *25*, 859-872.

(39) Lobban, C. S.; Harrison, P. J. *Seaweed ecology and physiology*; Cambridge University Press: Cambridge, 1994.

(40) Atkinson, R.; Baulch, D. L.; Cox, R. A.; Crowley, J. N.; Hampson, R. F.; Hynes, R. G.; Jenkin, M. E.; Rossi, M. J.; Troe, J. Evaluated kinetic and photochemical data for atmospheric chemistry: Volume III – gas phase reactions of inorganic halogens. *Atmos. Chem. Phys.* **2007**, *7*, 981-1191.

(41) Monahan, C.; Ashu-Ayem, E. R.; Nitschke, U.; Darby, S. B.; Smith, P. D.; Stengel, D. B.; Venables, D. S.; O'Dowd, C. D. Coastal Iodine Emissions: Part 2. Particle Nucleation Processes. *Environ. Sci. Technol.* **2012**, (Submitted).

(42) Gómez-Martín, J. C.; Ashworth, S. H.; Mahajan, A. S.; Plane, J. M. C. Photochemistry of OIO: Laboratory study and atmospheric implications. *Geophys. Res. Lett.* **2009**, *36*, 1-4.

(43) Ashworth, S. H.; Allan, J.; Plane, J. M. C. High resolution spectroscopy of the OIO radical: Implications for the ozone-depleting potential of iodine. *Geophys. Res. Lett.* **2002**, *29*, 1-4.

(44) Joseph, D. M.; Ashworth, S. H.; Plane, J. M. C. The absorption cross-section and photochemistry of OIO. *Photochem. Photobiol. A* **2005**, *176*, 68-77.

(45) Gómez-Martín, J. C.; Spietz, P.; Burrows, J. P. Kinetic and mechanistic studies of the I_2/O_3 photochemistry. *J. Phys. Chem. A* **2007**, *111*, 306-20.

(46) Harwood, M. H.; Burkholder, J. B.; Hunter, M.; Fox, R. W.; Ravishankara, A. R. Absorption cross sections and self-reaction kinetics of the IO radical. *J. Phys. Chem. A* **1997**, *101*, 853-863.

(47) Stutz, J.; Pikelnaya, O.; Hurlock, S. C.; Trick, S.; Pechtl, S.; von Glasow, R. Daytime OIO in the Gulf of Maine. *Geophys. Res. Lett.* **2007**, *34*, 3-7.

(48) Huang, R.-J.; Seitz, K.; Buxmann, J.; Pöhler, D.; Hornsby, K. E.; Carpenter, L. J.; Platt, U.; Hoffmann, T. In situ measurements of molecular iodine in the marine boundary layer: the link to macroalgae and the implications for O_3, IO, OIO and NO_x. *Atmos. Chem. Phys.* **2010**, *10*, 4823-4833.

TOC graphic